Geometrical edge barriers and magnetization in superconducting strips with slits

Yasunori Mawatari
Energy Electronics Institute, National Institute of Advanced Industrial Science and Technology, Tsukuba, Ibaraki 305-8568, Japan

John R. Clem
Ames Laboratory and Department of Physics and Astronomy, Iowa State University, Ames, Iowa 50011-3160, USA
(Received 6 February 2003; revised manuscript received 15 May 2003; published 17 July 2003)

We theoretically investigate the magnetic-field and current distributions for coplanar superconducting strips with slits in an applied magnetic field H_a. We consider ideal strips with no bulk pinning and calculate the hysteretic behavior of the magnetic moment m_y as a function of H_a due solely to geometrical edge barriers. We find that the m_y-H_a curves are strongly affected by the slits. In an ascending field, the m_y-H_a curves exhibit kink or peak structures, because the slits prevent penetration of magnetic flux. In a descending field, m_y becomes positive, because magnetic flux is trapped in the slits, in contrast to the behavior of a single strip without slits, for which $m_y \approx 0$.

DOI: 10.1103/PhysRevB.68.024505 PACS number(s): 74.25.Op, 74.25.Qt, 74.25.Ha, 74.78.−w

I. INTRODUCTION

Superconducting flat strips subjected to a perpendicular magnetic field show magnetic hysteresis, even when the strips have no bulk pinning. The magnetic hysteresis of strips without bulk pinning arises from geometrical edge barriers, i.e., barriers for magnetic-flux penetration at the strip edges.[1–6] Current-carrying strips have finite critical currents arising from the edge barriers,[7] and the critical current becomes larger when slits are fabricated near the edges of the strips.[8] The critical-current increase is due to the enhancement of edge-barrier effects; in other words, making slits increases the number of edges that prevent flux penetration into the inner strips. The reversible magnetic response of two strips (i.e., a strip with a slit) in the Meissner state was considered in Refs. 9 and 10. When an applied magnetic field exceeds a certain value, magnetic flux penetrates into the strips and the magnetic response becomes irreversible and hysteretic.[9]

In this paper, we present a theoretical investigation of the magnetic hysteresis of bulk-pinning-free strips with slits in the presence of an applied magnetic field H_a. The hysteretic behavior of the magnetic moment m_y as a function of H_a shown in this paper is due solely to the geometrical edge barriers. In Sec. II we outline our theoretical approach and establish notation. In Sec. III we briefly review published results of the m_y-H_a curves of a single strip without slits. In Sec. IV we investigate field distributions and m_y-H_a curves of two strips (i.e., a strip with a slit), and in Sec. V we study three strips (i.e., a strip with two slits). We briefly summarize our results in Sec. VI.

II. COMPLEX FIELD AND MAGNETIC MOMENT

We investigate coplanar superconducting strips (i.e., strips in which slits are fabricated parallel to the edges) in a perpendicular magnetic field but carrying no net transport current. The strips under consideration have total width $2a$, thickness $d \ll 2a$, and infinite length along the z axis (i.e., $|x|<a$ and $|y|<d/2$), as shown in Fig. 1. We assume that magnetic flux penetrates and escapes along the x axis, assuming that there is no flux penetration from the ends at $|z| \to \infty$. (We may think of the strip ends as being connected by superconducting shunts.)

The Biot-Savart law for the complex field[3,8,10,11] $\mathcal{H}(\zeta) = H_y(x,y) + iH_x(x,y)$ as a function of $\zeta = x+iy$ in the thin-strip limit $d/a \to 0$ is expressed as

$$\mathcal{H}(\zeta) = H_a + \frac{1}{2\pi}\int_{-a}^{+a} du \frac{K_z(u)}{\zeta - u}, \tag{1}$$

where the magnetic field H_a is applied parallel to the y axis, and $K_z(x) = \int_{-d/2}^{+d/2} j_z(x,y)dy$ is the sheet current along the z axis. In Secs. IV and V we show distributions of magnetic field $H_y(x,0) = \mathrm{Re}[\mathcal{H}(x)]$ and current $K_z(x)/2 = \mp H_x(x, \pm 0) = \mp \mathrm{Im}[\mathcal{H}(x \pm i0)]$. The multipole expansion of Eq. (1) for $|\zeta|/a \to \infty$ is expressed as

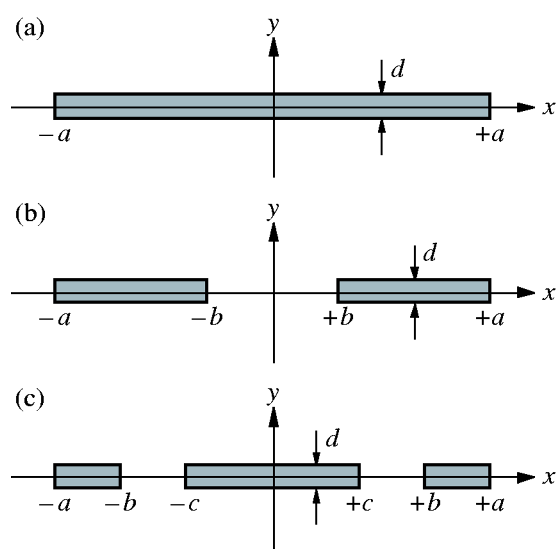

FIG. 1. Cross sections of strips with total width $2a$ and thickness d: (a) single strip without slit, (b) two strips (i.e., strip with a slit), and (c) three strips (i.e., strip with two slits).

 ©2003 The American Physical Society

$$\mathcal{H}(\zeta)\to H_a+\frac{1}{2\pi}\int_{-a}^{+a}duK_z(u)\left(\frac{1}{\zeta}+\frac{u}{\zeta^2}+\cdots\right)$$

$$\to H_a+\frac{I_z}{2\pi}\frac{1}{\zeta}-\frac{m_y}{2\pi}\frac{1}{\zeta^2}+\cdots, \tag{2}$$

where $I_z=\int_{-a}^{+a}dxK_z(x)$ is the transport current along the z axis and $m_y=\int_{-a}^{+a}dx(-x)K_z(x)$ is the magnetic moment in the y direction per unit length. In this paper we consider the hysteretic relationship between m_y and H_a of strips carrying no net current ($I_z=0$).

The complex field for symmetrically arranged strips has the general form [e.g., Eqs. (6), (14), and (34)]

$$\mathcal{H}(\zeta)=H_a\sqrt{\prod_n\frac{\zeta^2-\alpha_n^2}{\zeta^2-a_n^2}}, \tag{3}$$

where the strip edges are at $x=\pm a_n$. The parameter α_n generally depends on H_a. Equation (3) may be expanded as

$$\mathcal{H}(\zeta)\to H_a+\frac{H_a}{2\zeta^2}\sum_n(a_n^2-\alpha_n^2)+\cdots. \tag{4}$$

Comparing Eq. (4) with Eq. (2), we obtain a general expression for the magnetic moment per unit length [e.g., Eqs. (7), (15), and (35)],

$$m_y=-\pi H_a\sum_n(a_n^2-\alpha_n^2). \tag{5}$$

When H_a is small enough, such that the local magnetic fields at the strip edges are all less than the flux-entry field H_s,[4,7,8] the superconducting strips are in the Meissner state and no magnetic flux penetrates into the strips. References 9 and 10 describe the linear reversible magnetic response of two strips in the Meissner state. On the other hand, when H_a is sufficiently large to make the edge fields reach H_s, magnetic flux penetrates into the strips, and the magnetic response becomes irreversible and hysteretic. In Secs. III–V we determine the parameters α_n and the magnetic moment m_y as functions of H_a in ascending ($H_{a\uparrow}$) and descending ($H_{a\downarrow}$) fields.

III. SINGLE STRIP WITHOUT SLITS

A. Complex field for a single strip

In this section we consider a single strip of width $2a$, as shown in Fig. 1(a). The complex field $\mathcal{H}(\zeta)$ and the magnetic moment per unit length m_y for a single strip are given by[4]

$$\mathcal{H}(\zeta)=H_a\sqrt{\frac{\zeta^2-\alpha^2}{\zeta^2-a^2}}, \tag{6}$$

$$m_y=-\pi H_a(a^2-\alpha^2). \tag{7}$$

For convenience we introduce $a_\pm=a\pm\delta$, where δ is a cutoff length on the order of the thickness d when the penetration depth λ is small ($\lambda<d$) or the two-dimensional screening length $\Lambda=2\lambda^2/d$ when λ is large ($\lambda>d$); i.e., $\delta\sim\max(d,\Lambda)$.

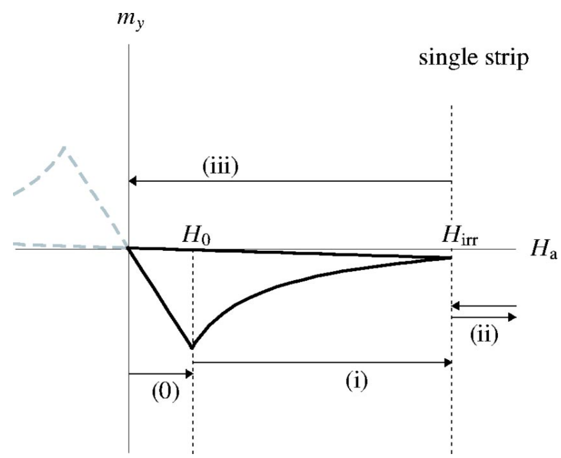

FIG. 2. Schematic of the magnetization curves, m_y versus H_a, for a single strip. The vertical dashed lines correspond to the characteristic fields H_0 and $H_{\rm irr}$. The horizontal arrows show field-evolution steps of (0), (i), (ii), and (iii).

For a single strip, the field-evolution process proceeds in four steps, as shown in Fig. 2: step (0) for $0<H_{a\uparrow}<H_0$, step (i) for $H_0<H_{a\uparrow}<H_{\rm irr}$, step (ii) for $H_a>H_{\rm irr}$, and step (iii) for $0<H_{a\downarrow}<H_{\rm irr}$. Details of the field-evolution steps are described in the following Secs. III B and III C.

B. Single strip in an ascending field

Step (0) for $0<H_{a\uparrow}<H_0$. When a magnetic field H_a is increased after zero-field cooling, the superconducting strips are initially in the Meissner state. The magnetic field at the edges is less than the flux-entry field H_s [i.e., $H_y(a_+,0)<H_s$], and the edge barriers near $x\simeq\pm a$ prevent penetration of magnetic flux. In this step (0), the parameter in Eq. (6) is $\alpha=0$, and the magnetic moment is given by

$$m_y/\pi=-H_aa^2. \tag{8}$$

Magnetic flux cannot penetrate into the strips so long as $H_y(a_+,0)<H_s$ for $H_a<H_0$, but step (0) terminates when $H_y(a_+,0)=H_s$ at $H_a=H_0$,

$$\frac{H_0}{H_s}=\frac{\sqrt{a_+^2-a^2}}{a_+}\simeq\sqrt{\frac{2\delta}{a}}, \tag{9}$$

where the second equality is valid for $\delta/a\ll1$.

Step (i) for $H_0<H_{a\uparrow}<H_{\rm irr}$. When $H_a>H_0$, magnetic flux nucleates at $x\simeq\pm a$ and penetrates into the strip. A domelike distribution of magnetic flux exists for $|x|<\alpha_1$ and grows as H_a increases. The parameter $\alpha=\alpha_1$ in Eq. (6) is determined by $H_y(a_+,0)=H_s$,

$$\alpha_1^2=a_+^2-(H_s/H_a)^2(a_+^2-a^2)\simeq a^2-2\delta a[(H_s/H_a)^2-1]. \tag{10}$$

The magnetic moment is given by

$$m_y/\pi=-H_a(a^2-\alpha_1^2)\simeq2(H_a-H_s^2/H_a)a\delta. \tag{11}$$

Step (i) terminates when $\alpha_1 = a_-$ at $H_a = H_{\rm irr}$, where

$$\frac{H_{\rm irr}}{H_s} = \sqrt{\frac{a_+^2 - a^2}{a_+^2 - a_-^2}} = \sqrt{\frac{2a+\delta}{4a}} \simeq \frac{1}{\sqrt{2}}. \tag{12}$$

Step (ii) for $H_a > H_{\rm irr}$. The domelike distribution of magnetic flux expands to include almost all of the strip, and the strip's magnetic response is reversible for $H_a > H_{\rm irr}$. The edge field at $H_a = H_{\rm irr}$ is given by $H_y(a_+,0) \simeq H_s$.

C. Single strip in a descending field

Step (iii) for $0 < H_{a\downarrow} < H_{\rm irr}$. In a descending field, magnetic flux escapes from the strip, but a domelike distribution of magnetic flux remains in the strip. The detailed behavior of the field distributions and m_y in descending fields depends upon the treatment of edges of a strip.[3–5] Here we adopt a simple model and put $\alpha = a_-$, which results in a domelike distribution of magnetic flux for $|x| < a_-$ and a small but sharply peaked current density flowing in the vicinity of the edges, $a_- < |x| < a$. The magnetic moment is given by

$$m_y/\pi = -H_a(a^2 - a_-^2) \simeq -2H_a a\delta, \tag{13}$$

which qualitatively agrees with that predicted by more detailed investigations.[3–5]

Note that m_y takes a very small negative value (i.e., $0 < -m_y \ll H_s a^2$), because a single strip cannot trap any magnetic flux in a descending field. Geometric edge barriers in a single strip without slits do not prevent escape of magnetic flux. At $H_a = 0$ magnetic flux is entirely removed from a single strip, resulting in zero remanent magnetic moment $m_y = 0$ at $H_{a\downarrow} = 0$. For strips with slits, on the other hand, magnetic flux is trapped in the slits, and m_y becomes positive in descending fields, as we show in Secs. IV and V.

IV. TWO STRIPS (STRIPS WITH A SLIT)

A. Complex field for two strips

In this section we consider two strips (i.e., a strip with a single slit) of total width $2a$, as shown in Fig. 1(b). The superconducting strips are at $b < |x| < a$, and the slit is centered between the strips $|x| < b$. We assume that the two strips are connected at the ends ($|z| \to \infty$) by superconducting shunts, such that an applied magnetic field H_a induces a circulating current in the two strips $\int_{-a}^{-b} K_z dx = -\int_{+b}^{+a} K_z dx \neq 0$. General expressions for the complex field and the magnetic moment per unit length for two strips are given by[10]

$$\mathcal{H}(\zeta) = H_a \sqrt{\frac{(\zeta^2 - \alpha^2)(\zeta^2 - \beta^2)}{(\zeta^2 - a^2)(\zeta^2 - b^2)}}, \tag{14}$$

$$m_y = -\pi H_a(a^2 + b^2 - \alpha^2 - \beta^2). \tag{15}$$

In this section we use parameters $a_\pm = a \pm \delta$ and $b_\pm = b \pm \delta$ [where $\delta \sim \max(d,\Lambda)$], and define the function $f_2(x) = (x^2 - a^2)(x^2 - b^2)$ for convenience.

For two strips, the field-evolution process proceeds in seven steps, as shown in Fig. 3: step (0) for $0 < H_{a\uparrow} < H_0$, step (i) for $H_0 < H_{a\uparrow} < H_1$, step (ii) for $H_1 < H_{a\uparrow} < H_{\rm irr}$, step (iii) for $H_a > H_{\rm irr}$, step (iv) for $H_4 < H_{a\downarrow} < H_{\rm irr}$, step (v) for $H_5 < H_{a\downarrow} < H_4$, and step (vi) for $-H_1 < H_{a\downarrow} < H_5$. Details of the field-evolution steps are described in the following Secs. IV B and IV C.

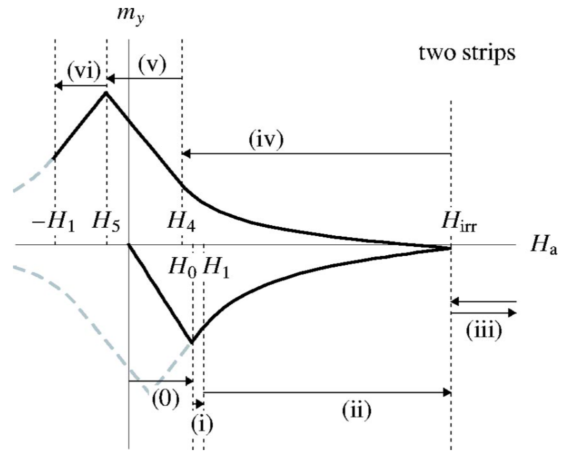

FIG. 3. Schematic of the magnetization curves, m_y versus H_a, for two strips. The vertical dashed lines correspond to the characteristic fields H_0, H_1, $H_{\rm irr}$, H_4, H_5, and $-H_1$. The horizontal arrows show field-evolution steps of (0), (i), (ii), (iii), (iv), (v), and (vi).

B. Two strips in an ascending field

Step (0) for $0 < H_{a\uparrow} < H_0$. When a magnetic field H_a is applied after zero-field cooling, the superconducting strips are initially in the Meissner state. The magnetic fields at the edges are less than the flux-entry field $0 < -H_y(b_-,0) < H_y(a_+,0) < H_s$ and no magnetic flux penetrates into the strips. Figure 4(a) shows distributions of the perpendicular field $H_y(x,0)$ and current $K_z(x)/2 = \mp H_x(x,\pm 0)$ in step (0). The parameters in Eq. (14) are given by $\alpha = \beta = \alpha_0 < b$. Because the total magnetic flux in the slit is zero, $\int_{-b}^{+b} H_y(x,0)dx = 0$, the parameter α_0 is determined as

$$\alpha_0^2 = a^2[1 - E(b/a)/K(b/a)], \tag{16}$$

where $K(k)$ and $E(k)$ are the complete elliptic integrals of the first and second kind, respectively. The magnetic moment is given by

$$m_y/\pi = -H_a(a^2 + b^2 - 2\alpha_0^2). \tag{17}$$

Step (0) terminates when $H_y(a_+,0) = H_s$ at $H_a = H_0$, where

$$\frac{H_0}{H_s} = \frac{\sqrt{f_2(a_+)}}{a_+^2 - \alpha_0^2} \simeq \frac{\sqrt{2\delta a(a^2 - b^2)}}{a^2 - \alpha_0^2}. \tag{18}$$

Step (i) for $H_0 < H_{a\uparrow} < H_1$. During this step, magnetic flux nucleates at the outer edges ($x = \pm a$), flows inward across the strips, and penetrates into the slit. Thus, we have $H_y(a_+,0) = H_s$ and $\int_{-b}^{+b} H_y(x,0)dx > 0$. The field distribu-

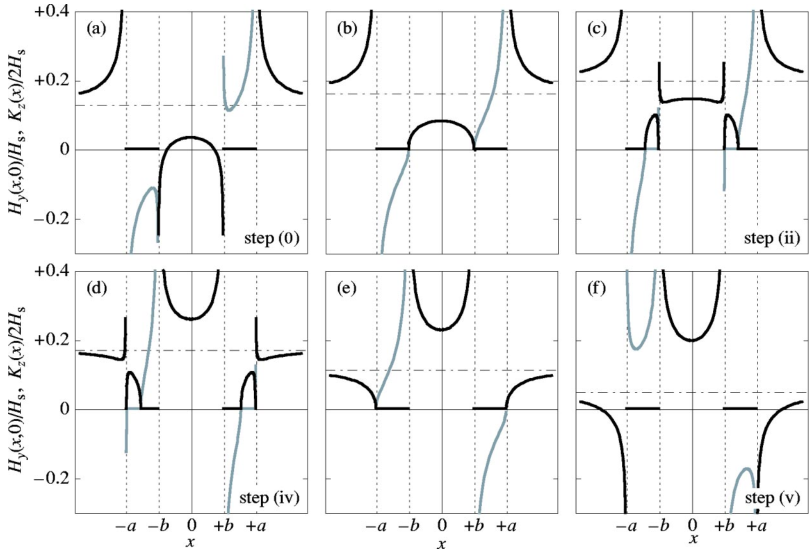

FIG. 4. Field distributions of $H_y(x,0)$, shown as black lines, and $K_z(x)/2=\mp H_x(x,\pm 0)$, shown as gray lines, in two strips for which $b/a=0.5$: (a) $0<H_{a\uparrow}<H_0$, (b) $H_{a\uparrow}=H_1$, (c) $H_1<H_{a\uparrow}<H_{\mathrm{irr}}$, (d) $H_4<H_{a\downarrow}<H_{\mathrm{irr}}$, (e) $H_{a\downarrow}=H_4$, and (f) $H_5<H_{a\downarrow}<H_4$. The horizontal dot-dashed lines show the applied magnetic field H_a.

tions in step (i) are similar to those in Fig. 4(a). The parameter $\alpha=\beta=\alpha_1$ is determined by $H_y(a_+,0)=H_s$,

$$\alpha_1^2=a_+^2-(H_s/H_a)\sqrt{f_2(a_+)}\simeq a^2-(H_s/H_a)\sqrt{2\,\delta a(a^2-b^2)}. \tag{19}$$

The magnetic moment m_y is given by

$$m_y/\pi=-H_a(a^2+b^2-2\alpha_1^2)$$
$$\simeq H_a(a^2-b^2)-2H_s\sqrt{2\,\delta a(a^2-b^2)}. \tag{20}$$

Step (i) terminates when $\alpha_1=b_+$ at $H_a=H_1$, where

$$\frac{H_1}{H_s}=\frac{\sqrt{f_2(a_+)}}{a_+^2-b_+^2}\simeq\sqrt{\frac{2\,\delta a}{a^2-b^2}}. \tag{21}$$

The field distribution at $H_a=H_1$ is shown in Fig. 4(b).

Step (ii) for $H_1<H_{a\uparrow}<H_{\mathrm{irr}}$. During this step, magnetic flux penetrates from $x=\pm a$, because $H_y(a_+,0)=H_s$. Domelike distributions of magnetic flux appear in the strips at $b_+<|x|<\alpha_2$ [Fig. 4(c)], and grow as H_a increases. Magnetic flux simultaneously exits the superconducting strips at $x=\pm b$ and enters the slit. Current spikes occur near $x\simeq\pm b$ in Fig. 4(c) because a finite current $K_z\neq 0$ flows in the vicinity of the inner edges, $b<|x|<b_+$, whereas $K_z=0$ for $b_+<|x|<\alpha_2$. In our theory, such current spikes, which produce wiggles in the local magnetic field distribution, always occur where magnetic flux is exiting from a dome in a superconducting strip.

The parameters are given by $\alpha=\alpha_2$ and $\beta=b_+$, where α_2 is determined by $H_y(a_+,0)=H_s$,

$$\alpha_2^2=a_+^2-\left(\frac{H_s}{H_a}\right)^2\frac{f_2(a_+)}{a_+^2-b_+^2}\simeq a^2-2\,\delta a[(H_s/H_a)^2-1]. \tag{22}$$

The magnetic moment m_y is given by

$$m_y/\pi=-H_a(a^2+b^2-\alpha_2^2-b_+^2)$$
$$\simeq-2(H_s^2/H_a)a\,\delta+2H_a(a+b)\,\delta. \tag{23}$$

Step (ii) terminates when $\alpha_2=a_-$ at the irreversibility field $H_a=H_{\mathrm{irr}}\simeq H_s/\sqrt{2}$, when domelike flux distributions essentially fill the strips. The domes occupy the regions $b_+<|x|<a_-$.

Step (iii) for $H_a>H_{\mathrm{irr}}$. When $H_a=H_{\mathrm{irr}}$, domelike flux distributions fill the regions $b_+<|x|<a_-$, and the magnetic response becomes reversible. At $H_a\simeq H_{\mathrm{irr}}$, the magnetic fields at the strip edges are $H_y(a_+,0)\simeq H_y(b_-,0)\simeq H_s$, and the parameters are given by $\alpha=a_-$ and $\beta=b_+$. The magnetic moment m_y, which is due to currents flowing in the narrow regions near the edges ($b<|x|<b_+$ and $a_-<|x|<a$), is given by

$$m_y/\pi=-H_{\mathrm{irr}}(a^2+b^2-a_-^2-b_+^2)\simeq-2H_{\mathrm{irr}}(a-b)\,\delta. \tag{24}$$

When $H_a>H_{\mathrm{irr}}$, the magnitude of m_y is reduced below that given in Eq. (24), because the current-carrying regions near the edges become narrower. However, a more detailed theory beyond the scope of the present approach would be required to calculate m_y for $H_a>H_{\mathrm{irr}}$.

C. Two strips in a descending field

Step (iv) for $H_4<H_{a\downarrow}<H_{\mathrm{irr}}$. If the applied field H_a has been above H_{irr} and now decreases through H_{irr}, magnetic flux is expelled from the slit and penetrates into the strips from the inner edge at $x=\pm b$, because the inner-edge field $H_y(b_-,0)$ is equal to the flux-entry field H_s. Magnetic flux in the strips escapes from the outer edges at $x=\pm a$. The domelike flux distributions at $\beta_4<|x|<a_-$ shrink as H_a decreases [Fig. 4(d)]. Current spikes occur near $x\simeq\pm a$ in Fig. 4(d) because a finite current $K_z\neq 0$ flows in the vicinity of the outer edges, $a_-<|x|<a$, whereas $K_z=0$ at $\beta_4<|x|<a_-$. The parameters are given by $\alpha=a_-$ and $\beta=\beta_4$, where β_4 is determined by $H_y(b_-,0)=H_s$,

$$\beta_4^2 = b_-^2 + \left(\frac{H_s}{H_a}\right)^2 \frac{f_2(b_-)}{a_-^2 - b_-^2} \simeq b^2 + 2\delta b[(H_s/H_a)^2 - 1]. \tag{25}$$

The magnetic moment m_y is given by

$$m_y/\pi = -H_a(a^2 + b^2 - a_-^2 - \beta_4^2)$$
$$\simeq 2(H_s^2/H_a)b\delta - 2H_a(a+b)\delta. \tag{26}$$

Step (iv) terminates and the domelike field distributions in the strips disappear when $\beta_4 = a_-$ at $H_a = H_4$ [Fig. 4(e)], where

$$\frac{H_4}{H_s} = \frac{\sqrt{f_2(b_-)}}{a_-^2 - b_-^2} \simeq \sqrt{\frac{2b\delta}{a^2 - b^2}}. \tag{27}$$

Step (v) for $H_5 < H_{a\downarrow} < H_4$. During this step, positive magnetic flux exits from the slit, penetrates into the strips from the inner edges at $x = \pm b$, flows outward entirely across the strips, and annihilates at the outer edges ($x = \pm a$), where $H_y(a_+, 0) < 0$. The field distribution is shown in Fig. 4(f).

The parameter $\alpha = \beta = \alpha_5$ is determined by $H_y(b_-, 0) = H_s$,

$$\alpha_5^2 = b_-^2 + (H_s/H_a)\sqrt{f_2(b_-)} \simeq b^2 + (H_s/H_a)\sqrt{2\delta b(a^2 - b^2)}. \tag{28}$$

Note that α_5 is real (and $\alpha_5 > a_-$) for $0 < H_a < H_4$, that $\alpha_5 \to \infty$ for $H_a \to +0$, and that α_5 is imaginary (i.e., $\alpha_5^2 < 0$) for $H_5 < H_a < 0$. The magnetic moment m_y is given by

$$m_y/\pi = -H_a(a^2 + b^2 - 2\alpha_5^2)$$
$$\simeq -H_a(a^2 - b^2) + 2H_s\sqrt{2\delta b(a^2 - b^2)}. \tag{29}$$

Even when $H_a < 0$, positive magnetic flux is still trapped in the slit, and the magnetic moment is positive.

Step (v) terminates when $H_y(a_+, 0) = -H_s$ at $H_a = H_5 < 0$,

$$\frac{-H_5}{H_s} = \frac{1}{a_+^2 - b_-^2}[\sqrt{f_2(a_+)} - \sqrt{f_2(b_-)}]$$
$$\simeq (\sqrt{a} - \sqrt{b})\sqrt{\frac{2\delta}{a^2 - b^2}}. \tag{30}$$

Step (vi) for $-H_1 < H_{a\downarrow} < H_5$. During this step, negative magnetic flux (i.e., flux lines aligned along the $-y$ axis) penetrates into the strips from the outer edges ($x = \pm a$), flows inward entirely across the strips, and annihilates at the inner edges ($x = \pm b$), where $H_y(b_-, 0) > 0$. The parameter $\alpha = \beta = \alpha_6$ is determined by $H_y(a_+, 0) = -H_s$, and is given by $\alpha_6(H_a) = \alpha_1(-H_a)$, where $\alpha_1(H_a)$ is defined in Eq. (19). Note that α_6 is imaginary (i.e., $\alpha_6^2 < 0$) for $H^* < H_a < H_5$, and that $0 < \alpha_6 < b_+$ for $-H_1 < H_a < H^*$, where H_1 is defined in Eq. (21) and

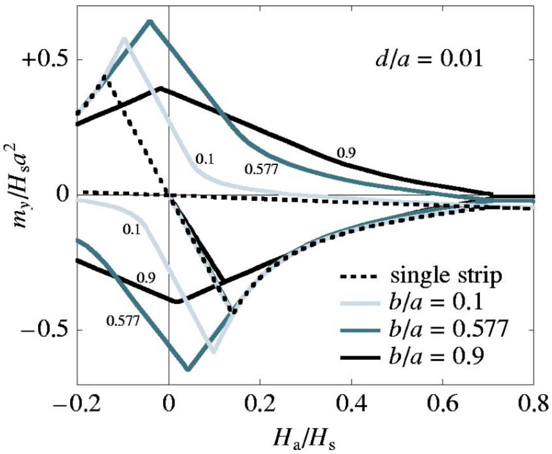

FIG. 5. Hysteretic behavior of the magnetic moment m_y of two strips as a function of the applied magnetic field H_a. Magnetization curves of a single strip (dashed lines) and two strips (solid lines) for $b/a = 0.1$, 0.577, and 0.9. The thickness of the strips is $d/a = 0.01$.

$$\frac{-H^*}{H_s} = \frac{\sqrt{f_2(a_+)}}{a_+^2} \simeq \sqrt{\frac{2(a^2 - b^2)\delta}{a^3}}. \tag{31}$$

The magnetic field at the center of the slit, $\mathcal{H}(0) = H_y(0,0) = H_a\alpha\beta/ab$, obeys $\mathcal{H}(0) > 0$ for $H_{a\downarrow} > H^*$, and $\mathcal{H}(0) < 0$ for $H_{a\downarrow} < H^*$.

Behavior for $H_{a\downarrow} < -H_1$. The magnetic response of two strips for $H_{a\downarrow} < -H_1$ in descending fields is very similar to the response for $H_{a\uparrow} > H_1$ in ascending fields. The complex field $\mathcal{H}(\zeta, H_a)$ and magnetic moment $m_y(H_a)$ in descending field can be determined from the ascending-field results with the help of the symmetries $\mathcal{H}(\zeta, H_{a\downarrow}) = -\mathcal{H}(\zeta, -H_{a\uparrow})$ and $m_y(H_{a\downarrow}) = -m_y(-H_{a\uparrow})$, respectively.

D. Magnetization curves of two strips

Figure 5 shows hysteretic m_y versus H_a curves for two strips. In ascending fields $H_{a\uparrow}$, the sheet current $K_z(x)$ concentrates near the outer edges of the strips at $x \simeq \pm a$ [Figs. 4(b) and 4(c)], and therefore, even for large b/a, the m_y for two strips is almost the same as that for a single strip except at low fields, $H_a/H_s \lesssim 0.2$.

In descending magnetic fields $H_{a\downarrow}$, we see in Fig. 5 a striking difference between $m_y > 0$ for two strips and $m_y \approx 0$ (i.e., $0 < -m_y \ll H_s a^2$) for a single strip. The inner edges of the two strips at $x = \pm b$ are responsible for the large positive magnetic moment. The edge barriers near $x = \pm b$ prevent magnetic-flux penetration from the slit region $|x| < b$ into the superconducting region $b < |x| < a$. Magnetic flux is therefore trapped in the slit as shown in Figs. 4(d)–4(f), and the magnetic moment becomes positive ($m_y > 0$).

The remanent magnetic moment $m_{\rm rem}$ is given by Eq. (29) with $H_a = 0$,

$$m_{\rm rem}/\pi \simeq 2H_s\sqrt{2\delta b(a^2 - b^2)}, \tag{32}$$

which is maximized when $b/a = 1/\sqrt{3} \approx 0.577$. If the slit is made wider, $m_{\rm rem}$ increases as b/a increases for $0 < b/a$

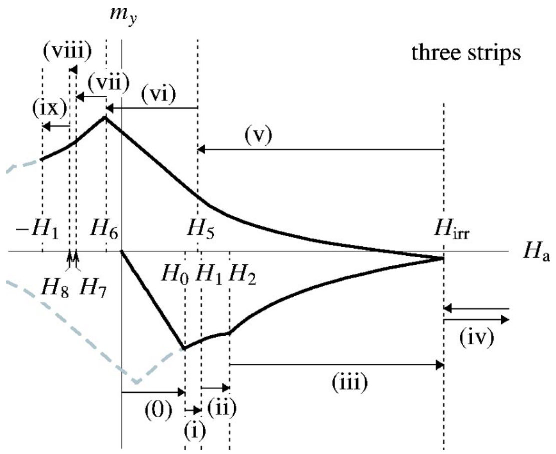

FIG. 6. Schematic of the magnetization curves, m_y versus H_a, for three strips. The vertical dashed lines correspond to the characteristic fields H_0, $H_1=(H_{1A}$ or $H_{1B})$, $H_2=(H_{2A}$ or $H_{2B})$, $H_{\rm irr}$, H_5, H_6, H_7, H_8, and $-H_1$. The horizontal arrows show field-evolution steps of (0), (i), (ii), (iii), (iv), (v), (vi), (vii), (viii), and (ix). The step (ii) corresponds to either (ii-A) when $b^2<a^2-ac+c^2$ or (ii-B) when $b^2>a^2-ac+c^2$.

$<1/\sqrt{3}$, because the slit can trap a larger amount of magnetic flux. If the slit is too wide, however, $m_{\rm rem}$ decreases for $1/\sqrt{3}<b/a<1$, because the superconducting strips (i.e., the current-carrying region) become too narrow. A similar behavior occurs for the peak of the magnetic moment $m_{\rm peak}$, which occurs at $H_a=H_5$. Equations (29) and (30) yield

$$m_{\rm peak}/\pi \simeq H_s(\sqrt{a}+\sqrt{b})\sqrt{2(a^2-b^2)\delta}, \tag{33}$$

which is maximized when $b/a\approx 0.403$.

V. THREE STRIPS (STRIPS WITH TWO SLITS)

A. Complex field for three strips

In this section we consider three strips (i.e., strips with two slits) of total width $2a$, as shown in Fig. 1(c). The outer strips are at $b<|x|<a$, the inner strip is at $|x|<c$, and the slits are at $c<|x|<b$. The strips are connected at the ends, $|z|\to\infty$, so that a circulating current flows in the outer strips, $\int_{-a}^{-b}K_z dx=-\int_{+b}^{+a}K_z dx\neq 0$. The inner strip carries no net current, $\int_{-c}^{+c}K_z dx=0$. The general expressions for the complex field and the magnetic moment per unit length for three strips are

$$\mathcal{H}(\zeta)=H_a\sqrt{\frac{(\zeta^2-\alpha^2)(\zeta^2-\beta^2)(\zeta^2-\gamma^2)}{(\zeta^2-a^2)(\zeta^2-b^2)(\zeta^2-c^2)}}, \tag{34}$$

$$m_y=-\pi H_a(a^2+b^2+c^2-\alpha^2-\beta^2-\gamma^2). \tag{35}$$

In this section we use parameters $a_\pm=a\pm\delta$, $b_\pm=b\pm\delta$, and $c_\pm=c\pm\delta$, where $\delta\sim\max(d,\Lambda)$. We also define a function $f_3(x)=(x^2-a^2)(x^2-b^2)(x^2-c^2)$ for convenience.

For three strips, the field-evolution process proceeds in ten steps, as shown in Fig. 6: step (0) for $0<H_{a\uparrow}<H_0$, step (i) for $H_0<H_{a\uparrow}<H_1=(H_{1A}$or $H_{1B})$, step (ii) for $H_1<H_{a\uparrow}<H_2=(H_{2A}orH_{2B})$, step (iii) for $H_2<H_{a\uparrow}<H_{\rm irr}$, step (iv) for $H_a>H_{\rm irr}$, step (v) for $H_5<H_{a\downarrow}<H_{\rm irr}$, step (vi) for $H_6<H_{a\downarrow}<H_5$, step (vii) for $H_7<H_{a\downarrow}<H_6$, step (viii) for $H_8<H_{a\downarrow}<H_7$, and step (ix) for $-H_1<H_{a\downarrow}<H_8$. Note that the step (ii) corresponds to either (ii-A) for $H_{1A}<H_{a\uparrow}<H_{2A}$ when $b^2<a^2-ac+c^2$, or (ii-B) for $H_{1B}<H_{a\uparrow}<H_{2B}$ when $b^2>a^2-ac+c^2$. Details of the field-evolution steps are described in the following Secs. V B and V C.

B. Three strips in an ascending field

Step (0) for $0<H_{a\uparrow}<H_0$. When a magnetic field H_a is applied after zero-field cooling [step (0)], the superconducting strips are initially in the Meissner state. Figure 7(a) shows the distributions of $H_y(x,0)$ and $K_z(x)/2=\mp H_x(x,\pm 0)$. The parameters in Eq. (34) are $\alpha=\beta=\alpha_0$ and $\gamma=0$, where $c<\alpha_0<b$. Because the net magnetic flux in the slits is zero, $\int_c^b H_y(x,0)dx=0$, we find that

$$\alpha_0^2=a^2-(a^2-c^2)\frac{E(k)}{K(k)},\quad k=\sqrt{\frac{b^2-c^2}{a^2-c^2}}. \tag{36}$$

The magnetic moment is

$$m_y/\pi=-H_a(a^2+b^2+c^2-2\alpha_0^2). \tag{37}$$

Step (0) terminates when $H_y(a_+,0)=H_s$ at $H_a=H_0$, where

$$\frac{H_0}{H_s}=\frac{\sqrt{f_3(a_+)}}{a_+(a_+^2-\alpha_0^2)}\simeq\frac{\sqrt{2\delta a(a^2-b^2)(a^2-c^2)}}{a(a^2-\alpha_0^2)}. \tag{38}$$

Step (i) for $H_0<H_{a\uparrow}<(H_{1A}$ or $H_{1B})$. In this step, magnetic flux nucleates at the outer edges, $x=\pm a$, flows inward across the outer strips, and penetrates into the slits; that is, $H_y(a_+,0)=H_s$ and $\int_c^b H_y(x,0)dx>0$. However, no magnetic flux penetrates into the inner strip because $H_y(c_+,0)<H_s$. The parameters are given by $\alpha=\beta=\alpha_1$ and $\gamma=0$, where $c<\alpha_1<b_+$. The value of α_1 is determined from $H_y(a_+,0)=H_s$,

$$\begin{aligned}\alpha_1^2&=a_+^2-(H_s/H_a)\sqrt{f_3(a_+)}/a_+\\&\simeq a^2-(H_s/H_a)\sqrt{2(a^2-b^2)(a^2-c^2)\delta/a}.\end{aligned} \tag{39}$$

The magnetic moment m_y is given by

$$\begin{aligned}m_y/\pi&=-H_a(a^2+b^2+c^2-2\alpha_1^2)\\&\simeq+H_a(a^2-b^2-c^2)-2H_s\sqrt{2(a^2-b^2)(a^2-c^2)\delta/a}.\end{aligned} \tag{40}$$

The sign of $dm_y/dH_a=\pi(a^2-b^2-c^2)$ can be either positive or negative, depending upon the relative widths of the strips.

Step (i) terminates when either $\alpha_1=b_+$ at $H_a=H_{1A}$ or $H_y(c_+,0)=H_s$ at $H_a=H_{1B}$. The characteristic fields H_{1A} and H_{1B} are given by

$$\frac{H_{1A}}{H_s}=\frac{\sqrt{f_3(a_+)}}{a_+(a_+^2-b_+^2)}\simeq\sqrt{\frac{2(a^2-c^2)\delta}{a(a^2-b^2)}}, \tag{41}$$

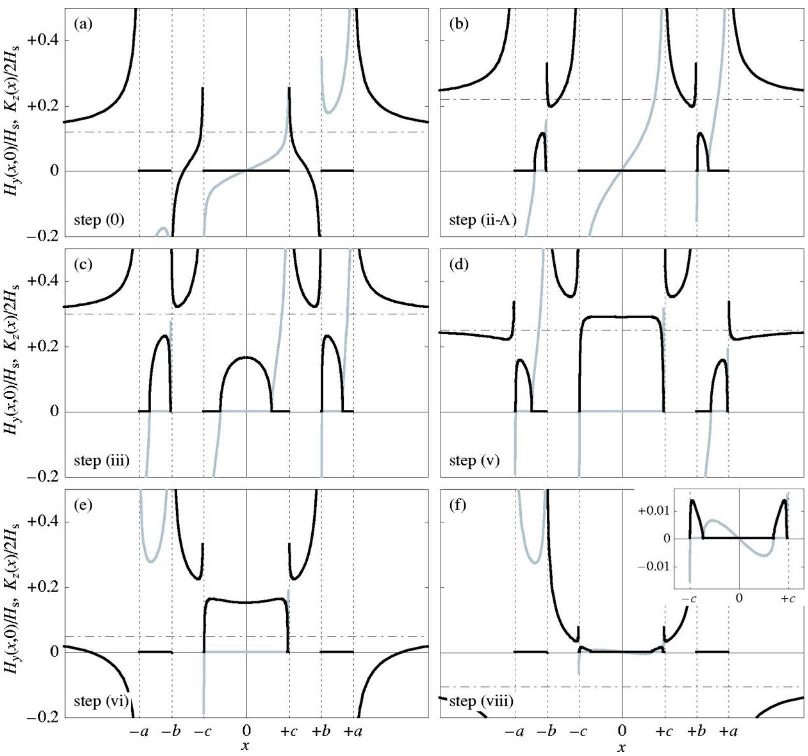

FIG. 7. Field distributions of $H_y(x,0)$, shown as black lines, and $K_z(x)/2=\mp H_x(x,\pm 0)$, shown as gray lines, in three strips for which $b/a=0.7$ and $c/a=0.4$: (a) $0<H_{a\uparrow}<H_0$, (b) $H_{1A}<H_{a\uparrow}<H_{2A}$, (c) $H_{2A}<H_{a\uparrow}<H_{\rm irr}$, (d) $H_5<H_{a\downarrow}<H_{\rm irr}$, (e)$H_6<H_{a\downarrow}<H_5$, and (f) $H_8<H_{a\downarrow}<H_7$ (magnified distribution in the inset). The horizontal dot-dashed lines show the applied magnetic field H_a.

$$\frac{H_{1B}}{H_s}=\frac{1}{a_+^2-c_+^2}\left[\frac{\sqrt{f_3(a_+)}}{a_+}+\frac{\sqrt{f_3(c_+)}}{c_+}\right]$$
$$\simeq\sqrt{\frac{2\delta}{a^2-c^2}}\left(\sqrt{\frac{a^2-b^2}{a}}+\sqrt{\frac{b^2-c^2}{c}}\right). \tag{42}$$

When $b^2<a^2-ac+c^2$, step (i) terminates at $H_a=H_{1A}<H_{1B}$, whereas when $b^2>a^2-ac+c^2$, step (i) terminates at $H_a=H_{1B}<H_{1A}$.

Step (ii-A) for $H_{1A}<H_{a\uparrow}<H_{2A}$ *and* $b^2<a^2-ac+c^2$. During this step, domelike distributions of magnetic flux are present at $b_+<|x|<\alpha_{2A}$ in the outer strips, whereas no magnetic flux penetrates into the inner strip [Fig. 7(b)]. The parameters are given by $\alpha=\alpha_{2A}$, $\beta=b_+$, and $\gamma=0$, where $b_+<\alpha_{2A}<a_-$, and α_{2A} is determined by $H_y(a_+,0)=H_s$,

$$\alpha_{2A}^2=a_+^2-\left(\frac{H_s}{H_a}\right)^2\frac{f_3(a_+)}{a_+^2(a_+^2-b_+^2)}$$
$$\simeq a^2-2(H_s/H_a)^2(a^2-c^2)\delta/a. \tag{43}$$

The magnetic moment m_y is given by

$$m_y/\pi=-H_a(a^2+b^2+c^2-\alpha_{2A}^2-b_+^2)$$
$$\simeq -H_a c^2-2(H_s^2/H_a)(a^2-c^2)\delta/a. \tag{44}$$

Step (ii-A) terminates when $H_y(c_+,0)=H_s$ at $H_a=H_{2A}$, where

$$\frac{H_{2A}}{H_s}=\sqrt{\frac{1}{a_+^2-c_+^2}\left[\frac{f_3(a_+)}{a_+^2(a_+^2-b_+^2)}+\frac{f_3(c_+)}{c_+^2(b_+^2-c_+^2)}\right]}$$
$$\simeq\sqrt{2(a+c)\delta/ac}. \tag{45}$$

Step (ii-B) for $H_{1B}<H_{a\uparrow}<H_{2B}$ *and* $b^2>a^2-ac+c^2$. In this step, a domelike distribution of magnetic flux is present for $|x|<\gamma_{2B}$ in the inner strip, whereas no magnetic flux is present in the outer strips. The parameters are given by $\alpha=\beta=\alpha_{2B}$ and $\gamma=\gamma_{2B}$, where $0<\gamma_{2B}<c_-$, $c<\alpha_{2B}<b$, and α_{2B} and γ_{2B} are determined by the coupled equations $H_y(a_+,0)=H_s$ and $H_y(c_+,0)=H_s$, which yield

$$H_s/H_a=(a_+^2-\alpha_{2B}^2)\sqrt{(a_+^2-\gamma_{2B}^2)/f_3(a_+)}$$
$$=(\alpha_{2B}^2-c_+^2)\sqrt{(c_+^2-\gamma_{2B}^2)/f_3(c_+)}. \tag{46}$$

The magnetic moment m_y is given by

$$m_y/\pi=-H_a(a^2+b^2+c^2-2\alpha_{2B}^2-\gamma_{2B}^2), \tag{47}$$

where α_{2B} and γ_{2B} must be determined numerically from Eq. (46). Step (ii-B) terminates when $\alpha_{2B}=b_+$ at $H_a=H_{2B}$, where

$$\frac{H_{2B}}{H_s}=\sqrt{\frac{1}{a_+^2-c_+^2}\left[\frac{f_3(a_+)}{(a_+^2-b_+^2)^2}-\frac{f_3(c_+)}{(b_+^2-c_+^2)^2}\right]}$$
$$\simeq\sqrt{\frac{2(a+c)(b^2-ac)\delta}{(a^2-b^2)(b^2-c^2)}}. \tag{48}$$

Step (iii) for $(H_{2A}$ *or* $H_{2B})<H_{a\uparrow}<H_{\rm irr}$. During this step, domelike distributions of magnetic flux are present both for

$|x|<\gamma_3$ in the inner strip and $b_+<|x|<\alpha_3$ in the outer strips [Fig. 7(c)]. The parameters are given by $\alpha=\alpha_3$, $\beta=b_+$, and $\gamma=\gamma_3$, where $0<\gamma_3<c_-$, $b_+<\alpha_3<a_-$, and α_3 and γ_3 are determined by the coupled equations $H_y(a_+,0)=H_s$ and $H_y(c_+,0)=H_s$, which yield

$$H_s/H_a=\sqrt{(a_+^2-\alpha_3^2)(a_+^2-\gamma_3^2)(a_+^2-b_+^2)/f_3(a_+)}$$
$$=\sqrt{(\alpha_3^2-c_+^2)(c_+^2-\gamma_3^2)(b_+^2-c_+^2)/f_3(c_+)}. \quad (49)$$

The magnetic moment is given by

$$m_y/\pi=-H_a(a^2+b^2+c^2-\alpha_3^2-b_+^2-\gamma_3^2)$$
$$\simeq 2H_a(a+b+c)\delta-2(H_s^2/H_a)(a+c)\delta. \quad (50)$$

Step (iii) terminates when $\alpha_3\simeq a_-$ and $\gamma_3\simeq c_-$ at $H_a=H_{\rm irr}\simeq H_s/\sqrt{2}$.

Step (iv) for $H_a>H_{\rm irr}$. The magnetic response is reversible for $H_a>H_{\rm irr}$. At $H_a=H_{\rm irr}$ the parameters are $\alpha=a_-$, $\beta=b_+$, and $\gamma=c_-$, and the magnetic fields at the edges are $H_y(a_+,0)\simeq H_y(b_-,0)\simeq H_y(c_+,0)\simeq H_s$. The magnetic moment at $H_a=H_{\rm irr}$ is given by

$$m_y/\pi=-H_{\rm irr}(a^2+b^2+c^2-a_-^2-b_+^2-c_-^2)$$
$$\simeq -2H_{\rm irr}(a-b+c)\delta. \quad (51)$$

C. Three strips in a descending field

Step (v) for $H_5<H_{a\downarrow}<H_{\rm irr}$. During this step, domelike distributions of magnetic flux are present for $\beta_5<|x|<a_-$ in the outer strips and for $|x|<c_-$ in the inner strip [Fig. 7(d)]. These domelike flux distributions shrink as H_a decreases. Magnetic flux escapes from the inner strip and penetrates into the slits. In turn, magnetic flux exits from the slits, penetrates into the outer strips, flows outward along the outer strips, and finally escapes from the strips at the outer edges, $x=\pm a$. The parameters are given by $\alpha=a_-$, $\beta=\beta_5$, and $\gamma=c_-$, where β_5 is determined by $H_y(b_-,0)=H_s$,

$$\beta_5^2=b_-^2+\left(\frac{H_s}{H_a}\right)^2\frac{f_3(b_-)}{(a_-^2-b_-^2)(b_-^2-c_-^2)}$$
$$\simeq b^2+2\delta b[(H_s/H_a)^2-1]. \quad (52)$$

The magnetic moment m_y is given by

$$m_y/\pi=-H_a(a^2+b^2+c^2-a_-^2-\beta_5^2-c_-^2)$$
$$\simeq -2H_a(a+b+c)\delta+2(H_s^2/H_a)b\delta. \quad (53)$$

Step (v) terminates when $\beta_5=a_-$ at $H_a=H_5$, where

$$\frac{H_5}{H_s}=\frac{1}{a_-^2-b_-^2}\sqrt{\frac{f_3(b_-)}{b_-^2-c_-^2}}\simeq\sqrt{\frac{2b\delta}{a^2-b^2}}. \quad (54)$$

Step (vi) for $H_6<H_{a\downarrow}<H_5$. Throughout this step, no magnetic flux remains in the outer strips, but a domelike distribution of magnetic flux is still present for $|x|<c_-$ in the inner strip [Fig. 7(e)]. Magnetic flux at $|x|<b$ penetrates into the outer strips from $x=\pm b$, flows outward entirely across the outer strips, and annihilates at $x=\pm a$, because $H_y(a_+,0)<0$. The parameters are given by $\alpha=\beta=\alpha_6$ and $\gamma=c_-$, where α_6 is determined by $H_y(b_-,0)=H_s$,

$$\alpha_6^2=b_-^2+\frac{H_s}{H_a}\sqrt{\frac{f_3(b_-)}{b_-^2-c_-^2}}\simeq b^2+(H_s/H_a)\sqrt{2\delta b(a^2-b^2)}. \quad (55)$$

Note that α_6 is real (and $\alpha_6>a$) for $0<H_a<H_5$, that $\alpha\to+\infty$ for $H_a\to+0$, and that α_6 is imaginary (i.e., $\alpha_6^2<0$) for $H_6<H_a<0$. The magnetic moment m_y is given by

$$m_y/\pi=-H_a(a^2+b^2+c^2-2\alpha_6^2-c_-^2)$$
$$\simeq -H_a(a^2-b^2)+2H_s\sqrt{2\delta b(a^2-b^2)}. \quad (56)$$

In the thin-strip limit $d/a\to 0$, the remanent magnetic moment $m_{\rm rem}$, given by Eq. (56) with $H_a=0$, is the same as for two strips, Eq. (32). Step (vi) terminates when $H_y(a_+,0)=-H_s$ at $H_a=H_6<0$, where

$$\frac{-H_6}{H_s}=\frac{1}{a_+^2-b_-^2}\left[\sqrt{\frac{f_3(a_+)}{a_+^2-c_-^2}}-\sqrt{\frac{f_3(b_-)}{b_-^2-c_-^2}}\right]$$
$$\simeq(\sqrt{a}-\sqrt{b})\sqrt{\frac{2\delta}{a^2-b^2}}. \quad (57)$$

Step (vii) for $H_7<H_{a\downarrow}<H_6<0$. During this step (not shown in Fig. 7), the magnetic field at the outermost edges is equal to the negative flux-entry field $H_y(a_+,0)=-H_s$. Negative magnetic flux penetrates into the outer strips at $x=\pm a$ and flows entirely across the outer strips into the slits, resulting in a reduction of magnetic flux in both the slits and the center strip. The parameter $\gamma=c_-$ is fixed, and $\alpha=\beta=\alpha_7$ is imaginary (i.e., $\alpha_7^2<0$), where α_7 is determined by $H_y(a_+,0)=-H_s$,

$$\alpha_7^2=a_+^2+\frac{H_s}{H_a}\sqrt{\frac{f_3(a_+)}{a_+^2-c_-^2}}\simeq a^2+(H_s/H_a)\sqrt{2\delta a(a^2-b^2)}. \quad (58)$$

The magnetic moment is given by

$$m_y/\pi=-H_a(a^2+b^2+c^2-2\alpha_7^2-c_-^2)$$
$$\simeq +H_a(a^2-b^2)+2H_s\sqrt{2\delta a(a^2-b^2)}. \quad (59)$$

Step (vii) terminates when $\alpha_7=0$ at $H_a=H_7<0$, where

$$\frac{-H_7}{H_s}=\frac{1}{a_+^2}\sqrt{\frac{f_3(a_+)}{a_+^2-c_-^2}}\simeq\sqrt{\frac{2(a^2-b^2)\delta}{a^3}}. \quad (60)$$

The magnetic field at the center, $\mathcal{H}(0)=H_y(0,0)$, is positive for $H_a>H_7$, but becomes zero at $H_a=H_7$.

Step (viii) for $H_8<H_{a\downarrow}<H_7<0$. During this step, domelike distributions of magnetic flux are present at $\beta_8<|x|<c_-$ in the inner strip, whereas no magnetic flux is present

in the inner region, $|x|<\beta_8$ [Fig. 7(f)]. The parameters are given by $\alpha=0$, $\beta=\beta_8$, and $\gamma=c_-$, where β_8 is determined by $H_y(a_+,0)=-H_s$,

$$\beta_8^2=a_+^2-\left(\frac{H_s}{H_a}\right)^2\frac{f_3(a_+)}{a_+^2(a_+^2-c_-^2)}$$
$$\simeq a^2-2(H_s/H_a)^2(a^2-b^2)\delta/a. \tag{61}$$

The magnetic moment is given by

$$m_y/\pi=-H_a(a^2+b^2+c^2-\beta_8^2-c_-^2)$$
$$\simeq -H_ab^2-2(H_s^2/H_a)(a^2-b^2)\delta/a. \tag{62}$$

Step (viii) terminates when $\beta_8=c_-$ at $H_a=H_8<0$, where

$$\frac{-H_8}{H_s}=\frac{\sqrt{f_3(a_+)}}{a_+(a_+^2-c_-^2)}\simeq\sqrt{\frac{2(a^2-b^2)\delta}{a(a^2-c^2)}}. \tag{63}$$

At $H_a=H_8$, no magnetic flux is present in either the inner or outer strips.

Step (ix) for $-H_1<H_{a\downarrow}<H_8<0$. During this step, no magnetic flux is present in the strips, and the parameters are given by $\alpha=0$ and $\beta=\gamma=\beta_9$. The parameter β_9, determined by $H_y(a_+,0)=-H_s$, is given by $\beta_9(H_a)=\alpha_1(-H_a)$, where α_1 is defined in Eq. (39).

Behavior for $H_{a\downarrow}<-H_1<0$. The magnetic response of two strips for $H_{a\downarrow}<-H_1$ in a descending field is very similar to that for $H_{a\uparrow}>H_1$ in an ascending field. The complex field and magnetic moment as functions of the applied field can be determined with the help of the symmetries $\mathcal{H}(\zeta,H_{a\downarrow})=-\mathcal{H}(\zeta,-H_{a\uparrow})$ and $m_y(H_{a\downarrow})=-m_y(-H_{a\uparrow})$, respectively.

D. Magnetization curves of three strips

Figure 8 shows hysteretic m_y-H_a curves for three strips. In ascending magnetic fields at $H_{a\uparrow}=(H_{2A}$ or $H_{2B})$, the m_y-H_a curves of three strips have additional kinks [see arrow in Fig. 8(a)] or peaks [see arrow in Fig. 8(b)]. Such kink or peak structures do not appear in the m_y-H_a curves for a single strip or two strips. They arise in three strips because the the edge barrier at the edges of the center strip ($x\simeq\pm c$) impede the entry of magnetic flux. In descending fields $H_{a\downarrow}$, on the other hand, the m_y-H_a curves for three strips are almost the same as those for two strips; the similarity occurs because the edges of the center strip do not impede the exit of magnetic flux.

In three strips, the edge barriers near $x\simeq\pm a$ and $\pm c$ are effective in preventing the entry of magnetic flux in $H_{a\uparrow}$, but are not effective in stopping the exit of magnetic flux in $H_{a\downarrow}$. On the other hand, while the edges at $x\simeq\pm b$ do not impede entering magnetic flux in $H_{a\uparrow}$, the edge barriers there are responsible for impeding flux exit in $H_{a\downarrow}$.

VI. CONCLUSION

We investigated field distributions and the magnetic moment m_y of bulk-pinning-free strips with slits in applied magnetic fields H_a, and we studied these in detail for increasing fields $H_{a\uparrow}$ and decreasing fields $H_{a\downarrow}$. For two strips, the complex field and the magnetic moment are given by Eqs. (14) and (15), respectively. The field-evolution process proceeds in seven steps, as shown in Fig. 3. In decreasing fields $H_{a\downarrow}$, the edge barriers near the inner edges at $x\simeq\pm b$ impede the exit of magnetic flux from the slit at $|x|<b$ into the strip at $b<|x|<a$. The trapping of magnetic flux in the slit in $H_{a\downarrow}$ results in a positive remanent magnetic moment, $m_y>0$ at $H_{a\downarrow}=0$, rather than a zero remanent moment, which occurs for a single strip without slits. For two strips, the remanent magnetic moment at $H_{a\downarrow}=0$ is maximized when $b/a=1/\sqrt{3}$.

For three strips (i.e., strips at $|x|<c$ and $b<|x|<a$), the complex field and the magnetic moment are given by Eqs. (34) and (35), respectively. The field-evolution process proceeds in ten steps, as shown in Fig. 6. The edge barriers at $x\simeq\pm b$ in $H_{a\downarrow}$ are effective in trapping magnetic flux as in two strips. In the thin-strip limit $d/a\to 0$, the remanent magnetic moment for three strips at $H_{a\downarrow}=0$ is the same as for two strips. In $H_{a\uparrow}$, the edge barriers at $x\simeq\pm c$ impede the penetration of magnetic flux into the inner strip. As a consequence, the m_y of three strips in $H_{a\uparrow}$ exhibits kink or peak structures that are not present for two strips.

The above arguments for three strips can be extended to an arbitrary number of strips. Consider a symmetric array of

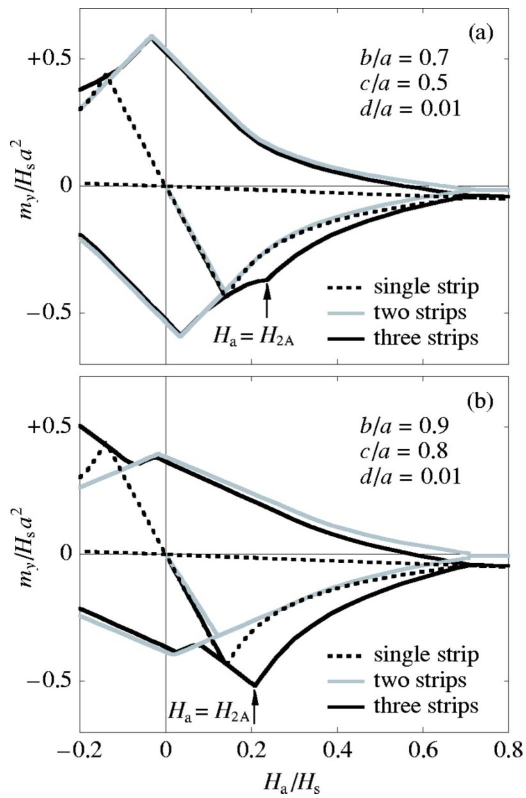

FIG. 8. Hysteretic behavior of the magnetic moment m_y of three strips as a function of the applied magnetic field H_a. (a) Magnetization curves of a single strip (dashed lines), two strips (gray solid lines) with $b/a=0.7$, and three strips (black solid lines) with $b/a=0.7$ and $c/a=0.5$. (b) Magnetization curves as (a) but for $b/a=0.9$ and $c/a=0.8$. The thickness of the strips is $d/a=0.01$.

N coplanar strips of total width $2a_0$ ($N-1$ slits), in which the strip edges are at $x=\pm a_n$, where $a_{N-1}<a_{N-2}<\cdots<a_1<a_0$. Superconducting strips occupy the regions $a_{n+1}<|x|<a_n$ with n even, and slits are at $a_{n+1}<|x|<a_n$ with n odd. The region spanning the centerline, $|x|<a_{N-1}$ corresponds to a superconducting strip for odd N and a slit for even N. The even edges at $x=\pm a_n$ for $n=0, 2, 4,\cdots$ impede flux entry in increasing applied fields $H_{a\uparrow}$, and the odd edges at $x=\pm a_n$ for $n=1, 3, 5,\cdots$ impede flux exit in decreasing fields $H_{a\downarrow}$.

By considering narrow slit widths, one may further extend the above approach to model grain-boundary pinning in thin films. The resulting model would be the thin-film analog of the bulk-pinning model discussed in Ref. 12.

ACKNOWLEDGMENTS

We thank H. Yamasaki for stimulating discussions. This work was done as a part of the Super-ACE project (a project for the R&D of fundamental technologies for superconducting ac power equipment) of the Ministry of Economy, Trade, and Industry of Japan. This manuscript has been authored in part by Iowa State University of Science and Technology under Contract No.W-7405-ENG-82 with the U.S. Department of Energy.

[1] M. V. Indenbom, H. Kronmüller, T. W. Li, P. H. Kes, and A. A. Menovsky, Physica C **222**, 203 (1994).
[2] Th. Schuster, M. V. Indenbom, H. Kuhn, E. H. Brandt, and M. Konczykowski, Phys. Rev. Lett. **73**, 1424 (1994).
[3] E. Zeldov, A. I. Larkin, V. B. Geshkenbein, M. Konczykowski, D. Majer, B. Khaykovich, V. M. Vinokur, and H. Shtrikman, Phys. Rev. Lett. **73**, 1428 (1994).
[4] M. Benkraouda and J. R. Clem, Phys. Rev. B **53**, 5716 (1996).
[5] T. B. Doyle, R. Labusch, and R. A. Doyle, Physica C **290**, 148 (1997).
[6] I. L. Maksimov and A. A. Elistratov, Appl. Phys. Lett. **72**, 1650 (1998).
[7] M. Benkraouda and J. R. Clem, Phys. Rev. B **58**, 15 103 (1998).
[8] Y. Mawatari and J. R. Clem, Phys. Rev. Lett. **86**, 2870 (2001).
[9] N. V. Zhelezina and G. M. Maksimova, Tech. Phys. Lett. **28**, 618 (2002).
[10] A. A. Babaei Brojeny, Y. Mawatari, M. Benkraouda, and J. R. Clem, Supercond. Sci. Technol. **15**, 1454 (2002).
[11] J. R. Clem, R. P. Huebener, and D. E. Gallus, J. Low Temp. Phys. **12**, 449 (1973).
[12] J. R. Clem, in *Low Temperature Physics - LT13*, edited by K. D. Timmerhaus, W. J. O'Sullivan, and E. F. Hammel (Plenum, New York, 1974), Vol. 3, p. 102.